OPTOELECTRONICS AND ADVANCED MATERIALS – RAPID COMMUNICATIONS Vol. 2, No. 6, June 2008, p. 332 - 336

Thermal behaviour study of the talc

K. BELGACEM[a*], PHI. LLEWELLYN, K. NAHDI[a], M.TRABELSI-AYADI[a]
MADIREL Laboratory, Provence University & CNRS13397 Marseille France.
[a] *LACReSNE Laboratory, University of Sciences, 7021 Bizerte, Tunisia*

Controlled transformation Rate Thermal Analysis (CRTA) has been used to study the thermal decomposition of a talc sample. The vacuum conditions and low rate of decomposition used in the present study has enabled to understand and quantify the decomposition in terms of the different brucite and talc sheets of the present mineral sample with chlorite impurity. Two mains decomposition steps at 500-650 °C and 650-1000 °C respectively were identified using CRTA, FTIR, XRD, SEM and BET analyses of heated talc at various temperatures. The first decomposition step, having the major duration, can be attributed to the deshydroxylation of the layers brucitic of chlorite while the second stage is due to the dehydroxylation of the layers mica (OH) of chlorite and of those of talc (OH). This result is in good agreement with the structure of both minerals (talc/chlorite) and also the arrangement of the hydroxyl groups.

(Received April 3, 2008; accepted June 4, 2008)

Keywords: Talc, Sample controlled thermal analysis, Chlorite

1. Introduction

The talc is a tri-octahedral layered mineral composed of hydrated magnesium silicate with the chemical formula $Mg_3Si_4O_{10}(OH)_2$. The talc structure consists of two tetrahedral silicate SiO_4 sheets separated by an octahedral $MgO_4(OH)_2$ sheet. Each tetrahedron shares three corners with the adjacent tetrahedrons. Therefore, three oxygen atoms of each tetrahedron belong simultaneously to two silicon atoms while the fourth oxygen atom belongs to one tetrahedral only. The ratio of the silicon to oxygen atoms is 2:5, thus corresponding to the formula $[Si_4O_{10}]^{4-}$. The charge of the anion layers is counter-balanced by the appropriate numbers of magnesium cations. Talc has found a wide-spread application such as rubber, paper, pharmaceutical, cosmetic, ceramic refractory and ceramic porcelain industries [1-3]. From an industrial standpoint therefore, the thermal decomposition behaviour of talc is of considerable interest. The dehydroxylation of pure talc, takes place as follows: $Mg_3(Si_2O_5)_2(OH)_2 = 3MgSiO_3 + SiO_2 + H_2O$ yielding enstatite, amorphous silica and water. However, as mineral, the talc contains also minor amounts of impurities like chlorites, dolomites, calcites, magnesites and quartz [4]. The composition and concentration of the talc depend on the paragenesis of the mineral. The influence of these impurities on the mechanical, thermal and electrical properties of the talc is very important for its final characteristics and applications.

Intensive studies by conventional thermoanalytical techniques (thermogravimetric analysis (TG), differential thermogravimetric analysis (DTG) and differential scanning calorimetry (DSC)) were carried out on the talc structure changes at various temperatures [11-19]. The analysed samples originated from locations throughout the world: Russian Federation [13], Germany [10], U.S.A [6], Japan [5], Taiwan [9], Pakistan [11], and India [12]. This fact explains why the descriptions of the thermal decomposition of talc are conflicting.

Many factors can have a significant effect on the results obtained by thermoanalytical methods. The different chemical composition of samples (it must be noted that talc minerals occurring in nature are rarely chemically pure substances) and the method/type of instrument used influence the shape of the thermograms. Furthermore conventional thermal analysis, which subjects samples to a linear heating rate, can have a major influence on the information content of the TG curve and the nature of the heat treated products.

To minimize as much as possible the influence of these parameters, the present study uses the method of Controlled Transformation Rate Thermal Analysis (CRTA) [17-19]. This method enables a control of the reaction rate allowing a sufficient decrease in the rate to diminish the pressure and temperature gradients within the reaction sample. The possibility of lowering the rate of transformation will makes it possible to ensure for the sample a more homogeneous temperature. The present investigation using CRTA was undertaken to clarify the dehydroxylation steps of sample of talc. Several intermediate samples were immediately analysed by XRD, FTIR and SEM with the aim to understand the decomposition mechanisms.

2. Experimental procedure

The talc investigated here comes from Tunisia. Firstly, the talc was characterized as purity and morphology. The chemical composition was determined by inductively coupled plasma-atomic emission spectrometry (ICP-AES) (Liberty 200, Varian, Clayton South, Australia). The microstructure of the talc powders was investigated using a Philips XL 30 scanning electron microscope. Nitrogen gas adsorption-desorption measurements using a nitrogen adsorption porosimeter

(Quanta-Chrome, Autosorb-1) were performed for talc powders to obtain their specific surface area. The granulometric distribution of the talc powder was measured on a LASER particle-measurement instrument (standard LS 130) using the optical model Fraunhofer. Sample Controlled Thermal Analyses were recorded by using a TA Instrument, model Q500 and an apparatus home built [17] respectively. The mixture of evolved gases is continuously analysed by a RIBER mass spectrometer coupled to the apparatus for Sample Controlled Thermal Analysis. FT-IR spectra were recorded in the 4000-400cm^{-1} range, using an EQUINOX 55 FTIR spectrometer (Bruker). The powder was pressed into KBr pellets. X-ray powder diffraction was investigated using a Siemens D 5000 X-ray diffractometer. CuKα1 radiation, (wavelength 1.5406 Å), a LiF crystal monochromator and Bragg-Brentano diffraction geometry were used.

3. Results and discussion

3.1. Chemical analysis

The chemical composition of the talc analysed by ICP-AES is presented in Table I.

Table I. Chemical composition of talc

Oxides	SiO_2	MgO	Al_2O_3	Fe_2O_3	CaO	P_2O_5	K_2O	TiO_2	MnO	Li_2O
Weight (%)	42.21	33.6	12.2	1.5	0.70	0.017	0.017	0.014	0.005	0.003

The result of the chemical analysis indicated high purity talc because the oxides considered as impurities (P_2O_5, K_2O, TiO_2, MnO, Li_2O) are present in very small amount (0.039%). Higher amount of CaO in talc mineral (0.70%) is usually for a mineral.

3.2. Talc decomposition

Thermal analysis (SCTA) and infrared spectroscopy (FT-IR) were used for better distinction of the steps and intermediate species that participate in the thermal transformations of the talc. The SCTA method provides a very slow thermal decomposition process. The CRTA curves of talc heated between 25 and 1000 °C are shown in Fig. 1.

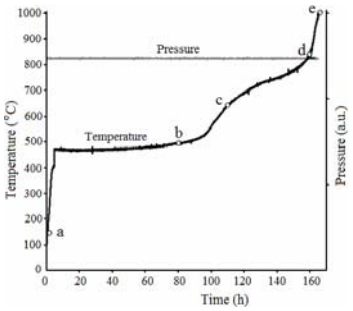

Fig.1. CRTA curves of the talc under 2·10^{-2} mbar water vapours pressure.

In this method, production rate of the gaseous phase can be permanently controlled (adjusting the heating rate) so that the pressure level above the sample could be kept at a reference value of ~ 2·10^{-2} mbar (curve "Pressure" in Fig.1). The time measured for each decomposition step is directly proportional to the weight loss. According to major changes suggested by the form of the temperature curve, we can divide the decomposition process into three steps. In order to obtain more information on the thermal decomposition of talc, a continuous evolved gas analysis was carried out during CRTA. These results are given in Fig.2 and Fig.2a.

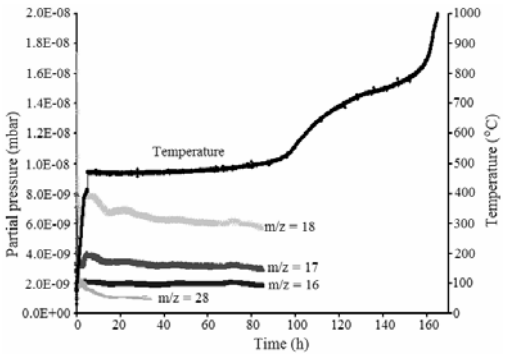

Fig.2. Mass spectrometric analyses of products out gassed from talc surface during the SCTA thermolysis.

SCTA analysis of the talc showed a first step until 200 ºC. The mass spectrum of the species evolved until 200 ºC (Fig.2 and Fig.2a) showed peaks at (*m*/*z*) = 16, 17, 18, and 28 mass/charge ratios. The peaks at *m*/*z* = 16, 17, 18, and 28 correspond to physically adsorbed water and, carbon dioxide and/or nitrogen respectively.

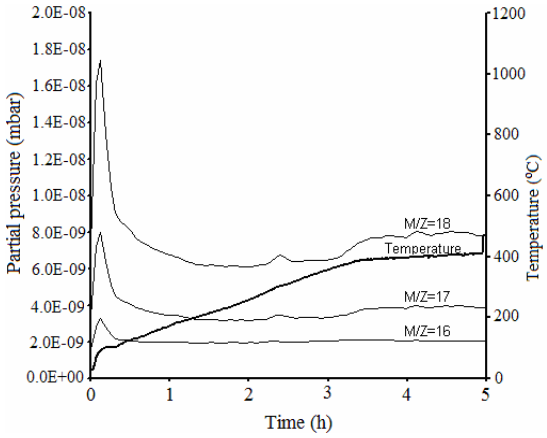

Fig.2a. Detail of the first field of Fig.2.

The next two steps occur between 500-650°C (I) and 650-1000°C (II), respectively, and are characterised by loss of the compositional water (m/z=18; 17, 16). The presence of OH groups (peaks m/z=18) at high

temperature suggests a continuous water loss from the talc by thermal decomposition.

To characterize the products obtained at the end of each decomposition step, the CRTA experiment was stopped at the temperatures determined from the initial curves: points (a) non-treated, as well as the intermediates treated to (b) 500°C, (c) 650°C, (d) 850°C and (e) 1000°C and restarted under identical conditions. These intermediate products are immediately submitted to IR, X-ray powder diffraction, SEM and BET studies.

The IR spectra of un-heated talc and of intermediate products of the thermal decomposition are presented in Fig.3.

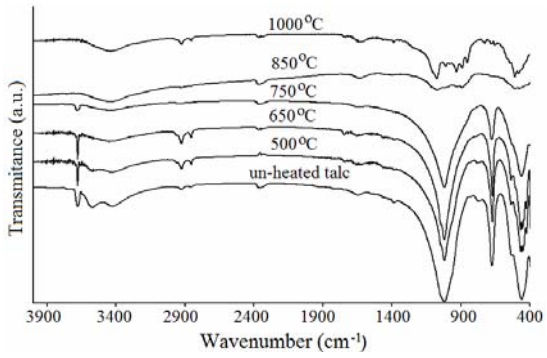

Fig.3. IR spectra of the talc and intermediate products obtained at different temperatures by thermolysis under $2 \cdot 10^{-2}$ mbar water vapours pressure.

The infrared spectra of the initial compounds clearly exhibits the presence of talc by the very sharp O-H stretching at 3674 cm^{-1} (which is badly overlapped by vibration of talc-like hydroxyl group stretching at 3670 cm^{-1}) and the sharp symmetric Si-O-Si stretching at 667 cm^{-1}. The asymmetric Si-O-Si stretching is observed at 1004 cm^{-1}.Whereas adsorption bands observed at 3562 and 3411 cm^{-1} correspond to the brucite layer hydroxyl group of chlorite. The appearance of these broad bands indicates the presence of chlorite in the sample. The absorption bands towards 812 and 727 cm^{-1} are attributed to the mode of vibration of (Si-Al) O-OH. The absorption bands between 401 and 514 cm^{-1} are attributed to the bending vibrations of Si-O. Change in the IR spectra appears up to 450 °C. At 650 °C the 3562 and 3411 cm^{-1} stretching bands of the brucitic hydroxyls of chlorite disappear. The stretching vibration of talc hydroxyls at 3674 cm^{-1} (which appears at 450 °C) disappears completely at 800 °C. Whereas in 1500-400 cm^{-1} range; dehydroxylation of the OH groups of interlayer octahedral sheet changes the Si-O stretching bands in the 1051-968 cm^{-1} range into one weak broad band which broadens between 500 and 750 °C (Fig.3). This could indicate short range disordering in the tetrahedral sheet of the 2:1 layer. This disorganization is further indicated by shoulders near 850 and 750 cm^{-1} which could be assigned to the modification of the tetrahedral Al-O environment as the 765 cm^{-1} vibration disappears after dehydroxylation. The 699 cm^{-1} band which startes to decrease at 750 °C, disappears completely at 850 °C while the 401-514 cm^{-1} bands are not affected. The spectrum IR of the product insulated at the end from thermolysis (at 1000 °C, Fig.3) reveals the bands characteristic of enstatite.

3.3. Microstructure

SEM images obtained for the isolated dehydrated talc shows that the crystal morphology was preserved after heat treatment by CRTA up to 700 °C (Figs. 4a-b).

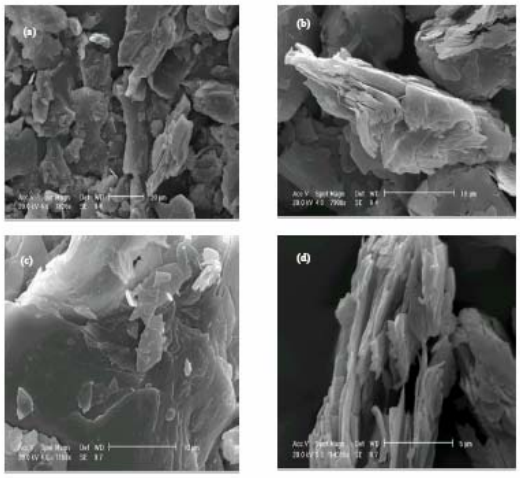

Fig.4. SEM images of the talc non heated (a) and heated at 650°C (b), 850°C (c) and 1000°C (d) by CRTA thermolysis under $2 \cdot 10^{-2}$ mbar water vapour pressure.

The observations indicate that the loss of water during the first step has or no a small effect on the lattice architecture. However SEM images obtained for products isolated at 850 and 1000 °C (Figs.4c-d) show large cracks on the surface indicating that the loss of the last water molecules degrades the crystal structure.

The analysis of the powder specific surface area for talcs heated at various temperatures was carried out using the BET method (Fig. 5).

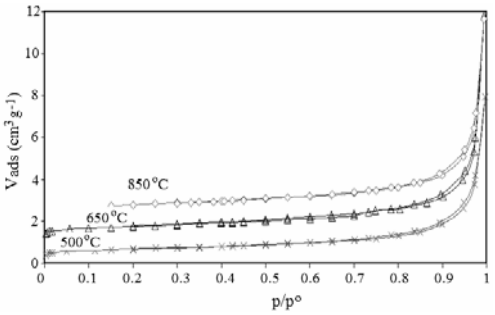

Fig.5. Nitrogen isotherms obtained at 77 K on intermediate samples isolated at 500 °C, 650 °C and 1000 °C.

Each isotherm shows "Type II behaviour" specific to the non-porous materials. A negligible amount of hysteresis is observed which may be due to non-rigid interparticle voids. Nevertheless, very few differences are observed between the unheated sample and the intermediate products at 500, 650 and 850 °C which all have close BET specific surface areas: 2.38, 2.48 and 2.45 (± 0.2) m^2g^{-1}. The specific surface ares of talc, measured by adsorption of nitrogen at 77 K, is equal to 2.43m^2g^{-1}. The grain size of the talc is about 10 µm.

3.4. Structure

The X-ray diffraction patterns of un-heated talc and intermediate products of the thermal decomposition process are presented in Fig. 5.

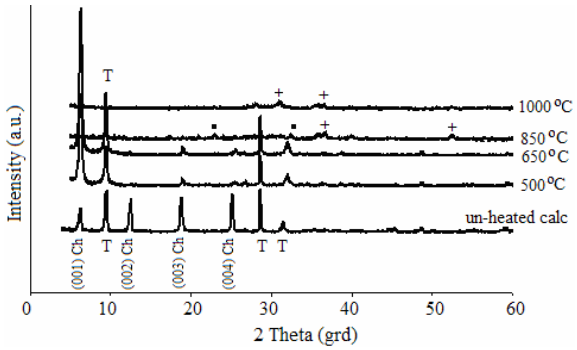

Fig.6. X-ray diffraction patterns of talc and of intermediate products obtained at different temperatures by thermolysis under $2 \cdot 10^{-2}$ mbar; T- talc, Ch – chlorite, (▪) - forsterite, (+) - enstatite.

The spectrum of the un-heated talc shows peaks corresponding to the talc and chlorite. Analysis of the pattern obtained for the initial sample shows an amount of about 66.3% chlorite. The diffractogram of the talc heated at 500 °C (Fig.6), indicates the disappearance of the 002 peak of chlorite and a strong attenuation of the other peaks (< 003 >, < 004 >) of chlorite phase. The intensity of the (001) peak of chlorite increases suggesting the dehydroxylation of the brucitic phase of chlorite [20]. The patterns of talc remain without modification at this temperature. The XRD patterns of the talc heated at 650 °C are identicaly with those of the talc calcined at 500 °C (Fig.6). For the sample heated at 850 °C, the peaks related to the talc and chlorite disappeared completely and new patterns corresponding to orthorhombic enstatite ($MgSiO_3$) [21] and fosterite (Mg_2SiO_4) [22] appear. The diffractogram of the talc calcinated at 1000 °C shows only the peaks corresponding to poorly crystalline enstatite phase. XRD analysis indicates that the decomposition of talc is complete at 1000 °C.

4. Conclusions

The complete dehydroxylation of talc was analyzed by CRTA, FTIR and XRD methods in 25-1000 ºC temperature region. The gas composition above the sample analyzed during the thermolysis of the talc confirmed the CRTA results.

The CRTA curves of the talc and the FTIR, XRD, SEM and BET analyses of heated talc at various temperatures, indicated two mains decomposition steps at 500-650 °C and 650-1000 °C respectively. The first decomposition step, having the major length, can be attributed to the dehydroxylation of the brucitic layers of chlorite while the second stage is due to the dehydroxylation of the mica (OH) layers of chlorite and of those of talc (OH).

This result is in good agreement with the structure of both minerals (talc/chlorite) as well as the arrangement of the hydroxyl groups. The elementary layer of talc is composed of an octahedral plane of brucite ($Mg(OH)_2$) with only one type of –OH site confined between two external tetrahedral silicate sheets. The chlorite is composed of alternating talc (containing two hydroxyl (OH) groups separated by bridging oxygen) and brucite layers containing six hydroxyl (OH) groups arranged close to each other. During the heating of the mineral, water is released in distinct steps due to differences in bonding energy.

The XRD analysis of the initial talc indicated a chlorite content of 66.3%.

This study shows the possibility to characterise, via CRTA, the mineral talc in terms of talc decomposition and the quantification of the secondary phase such as chlorite.

References

[1] L. A. Pérez-Maqueda, A. Duran, J. L. Pérez-Rodríguez, Clay Sci, **28** (1-4), 245 (2005).
[2] R.L. Johnson and R.L. Virta, Talc, Am. Ceram. Soc. Bull, **79**, 79 (2000).
[3] R.L. Johnson, Talc, Am. Ceram. Soc. Bull, **76**, 136 (1997).
[4] W. A. Deer, R. A. Howie, J. Zussman, Rock-Forming Minerals, V. 3, Longmans, London, p. 126, (1967).
[5] T. Stuo, K. Nagasawa, M. Amafuji, M. Kimura, S. Honda, Muto and M. Tanemura, J. Geol. Soc. Jpn., **58**, 115 (1952).
[6] P. D. Gran, S. S. Flaschen, Anal. Chem, **29**, 271 (1957).
[7] O. Bolgiu, A. Dumitrescu, Acad. Repub. Pop. Rom., Stud. Ceret. Met, **2**, 523 (1957).
[8] H. Gelly, Met., Corros. Ind., **32**, 214 (1957).
[9] S. Rosenblum, P. H. H. Lu, Proc. Geol. Soc. China, **2**, 147 (1959).
[10] F. Lippmann, Keram. Z., **11**, 750 (1957).
[11] M. A. Qaiser, M. K. Ali, A. H. Khan, Pak. J. Sci. Ind.

Res., **11**, 23 (1968)
[12] P. K. Chatterjee, D. P. Bahl, I. Ray, Rec .Geol. Surv. India, **105**, 139 (1973)
[13] P. P. Smolin, B. B. Zvyagin, V. A. Drits, O. V. Sidorenko, V. A.Aleksandrova, Dokl. Akad. Nauk SSSR, **218**, 924 (1974).
[14] I. Soos, Muanyag Gumi, **12**, 215 (1975).
[15] H. Koshimizu, S.H. Higuchi, R. Otsuka, Nendo Kagaku, **21**, 61 (1981)
[16] J. S. Venugopal, B. V. Hirannaiah, S. K. Majumder, J. Geol. Soc. India, **23**, 300 (1982).
[17] J. Rouquerol, Thermochim. Acta, **144**, 203 (1986)
[18] O. T. Sorensen, J. Rouquerol, (eds.), Sample controlled thermal analysis.Origin, goals, multiple forms, applications and future. (Kluwer Academic Publishers, Dordrecht, 2003) (Hot Topics in Thermal Analysis and Calorimetry, 3), 252 p
[19] F. Villieras, J. Yvan, J. M. Cases, J. L. Zimmermann, R. Beaza, Dosage et localisation du fer II dans le talc et la chlorite par analyse spectrométrique des gaz de thermolyse. Comptes Rendus de l'Académie des Sciences (Paris), **315**, 1201 (1992).
[20] H. W. Van der Marel, H. Beutelspacher, Atlas of Infrared spectroscopy of clay minerals and their Admixtures, 194 (Elsevier, Amsterdam, 1976).
[21] S. Sasaki, K. Fujino, Y. Takeuchi, P. Sadanaga, Acta Cryst. A, **36**, 904 (1980); JCPDS 30-523.
[22] S. Tamazaki, H. Toraya, J. Appl. Cryst., **32**, 51 (1999); JCPDS 88-023.

*Corresponding author: kaouther_fsm@yahoo.fr